



POLİTEKNİK DERGİSİ

JOURNAL of POLYTECHNIC

ISSN: 1302-0900 (PRINT), ISSN: 2147-9429 (ONLINE)

URL: <http://dergipark.org.tr/politeknik>



Frequency response of an initially stressed slab made from three compressible materials

Üç sıkıştırılabilir malzemedен yapılmış ön gerilmeli bir plakanın frekans tepkisi

Yazar(lar) (Author(s)): Ahmet DAŞDEMİR

ORCID: 0000-0001-8352-2020

Bu makaleye şu şekilde atıfta bulunabilirsiniz (To cite to this article): Daşdemir A., “Frequency response of an initially stressed slab made from three compressible materials”, *Politeknik Dergisi*, 24(1): 275-282, (2021).

Erişim linki (To link to this article): <http://dergipark.org.tr/politeknik/archive>

DOI: 10.2339/politeknik.650808

Frequency Response of an Initially Stressed Slab Made from Three Compressible Materials

Highlights

- ❖ A pre-stressed system consisting of three slabs side-by-side was modeled.
- ❖ The finite element solution procedure was presented for the considered problem.
- ❖ The frequency response of the slab caused by the time-harmonic force was investigated.
- ❖ The influence of the initial stress state on the dynamic response of the slab was observed.

Graphical Abstract

Presented herein is to model the dynamical behavior of the pre-stressed slab with three layers side-by-side resting on a rigid foundation under the action of a time-harmonic force. In particular, the dependency between the dimensionless frequency and initial stress parameters is investigated.

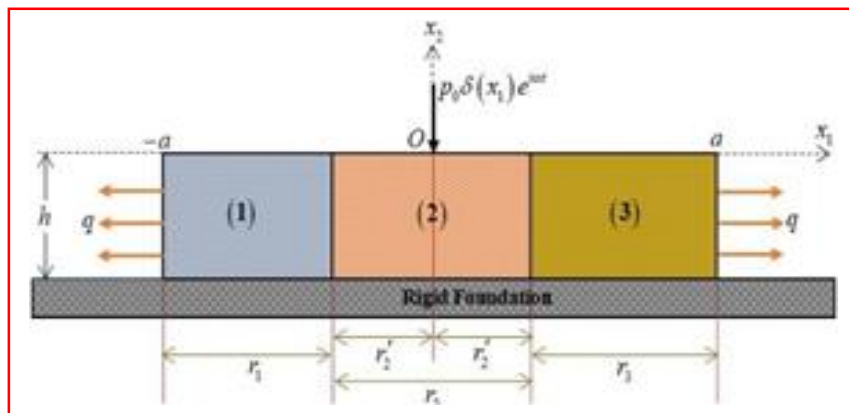


Figure. The system pattern

Aim

The paper reports on how to model for a pre-stressed slab with three different layers and analyses in which cases the system could in convenient form or not.

Design & Methodology

The model is carved out within the scope of the piecewise homogeneous body model utilizing the three-dimensional linearized theory of elastic waves in initially stressed bodies.

Originality

A dynamical stress field problem for an interface including three surfaces with different material properties was examined.

Findings

It is founded that the resonance values of the system decrease when the layer-length ratio increases. Besides, as the initial stress increase, the resonance mode of stress exceeds.

Conclusion

The layer-length ratio has a significant role in the influence of the frequency response of the slab. As the initial stresses increase, the system becomes a more stable form.

Declaration of Ethical Standards

The author of this article declares that the materials and methods used in this study do not require ethical committee permission and/or legal-special permission.

Üç Sıkıştırılabilir Malzemedan Yapılmış Ön Gerilmeli Bir Plakanın Frekans Tepkisi

Araştırma Makalesi / Research Article

Ahmet DAŞDEMİR*

Faculty of Arts and Sciences, Department of Mathematics, Kastamonu University, Turkey

(Geliş/Received : 25.11.2019 ; Kabul/Accepted : 19.03.2020)

ÖZ

Bu çalışmada, sert bir temel üzerinde duran ve zamana göre harmonik bir yükün etkisi altındaki ön gerilmeli bir levhanın frekans tepkisi ele alınmıştır. Araştırma, Ön Gerilmeli Ortamlarda Dalga Yayılımının Üç Boyutlu Doğrusallaştırılmış Teorisi (ÖODYÜT) kullanarak parçalı homojen cisim modeli göre gerçekleştirilir. Ele alınan cisim, üç ayrı plakanın yan yana birleştirilmesiyle oluşturulur. Sistemdeki tüm ara yüzey düzlemlerinde sert kenetlenme durumu olduğunu varsaydık. Problemin matematiksel bir modeli oluşturulur ve hareket denklemleriyle ilgili sistem sonlu elemanlar yöntemi (SEY) kullanılarak sayısal olarak çözülüyor. Özellikle, katman uzunluğunun oranının, plakanın frekans cevabı üzerindeki etkisi sunulmuştur.

Anahtar Kelimeler : Tam bağlı temas koşulu, sıkıştırılabilir malzeme, dinamik tepki, sonlu elemanlar yöntemi, başlangıç gerilmesi.

Frequency Response of an Initially Stressed Slab Made from Three Compressible Materials

ABSTRACT

In this study, the frequency response of a pre-stressed slab, which stands on a rigid foundation, subject to a timely harmonic loading was considered. The investigation is implemented according to the piecewise homogeneous body model utilizing the three-dimensional linearized theory of elastic waves in initially stressed bodies (TLTEWISB). The considered body was designed joining to three discrete slabs side-by-side. It was assumed that there exists a rigidly clamping state at all interface planes on the system. A mathematical model of the problem is constructed and the system related to equations of motion is numerically solved using the finite element method (FEM). Particularly, the effect the ratio of the layer length has on the frequency response of the slab was presented.

Keywords: Complete contact condition, compressible material, dynamic response, finite element method, initial stress.

1. INTRODUCTION

Sandwich structures are a composite material of three layers, i.e. two layers were bonded to a core layer. These materials have many applications in almost every field of metallurgical and engineering applications. This has encouraged dense research and risen significant attention to the subject. However, corresponding problems regarding the sandwich materials include many factors, thus making them difficult to solve these problems; more particularly, nonlinear wave propagation in the dynamics of the elastic phase might arise. Two of the factors that play a key role in the non-linear dynamic behavior of the considered body are (1) the initial stresses applied to the body, which exist before the dynamic load, and (2) choice of material to form the body, e.g. elastic or piezoelectric materials.

The first factor is one of the most important characters that are used in many engineering applications, due to either a technological process using for assembly or action of the environmental temperature. In general, the

initial stress state in the deformed system (including layers) cannot be examined according to the linear theory of elasticity, because this has a non-linear effect in the system. However, based on the assumption that the amplitude of the deformations caused by external forces in a pre-stressed medium is considerably less than that of the initial deformation, they can be investigated in terms of the three-dimensional linearized theory of elastic waves in initially stressed bodies (TLTEWISB); see the references in [1-3] for more detailed information on the subject. There are a number of the studies made according to the fundamental principles of the TLTEWISB and its other versions. For example, in [4], Wen-tao, et al. considered the effect of homogeneous initial pressures applied to the radial surfaces of a hollow cylinder. In [5], Daşdemir and Eröz investigated the effect of the pre-stress parameter on the dynamic behavior of a bi-layered plate-strip resting on a rigid foundation; however, this paper presents the numerical results including the case in which there is an initial tension force was the only case. Therefore, to address this issue, in [6], Daşdemir analyzed the effect of the initial compression force on the frequency response of the bi-layered system and compared the numerical findings

*Sorumlu Yazar (Corresponding Author)
e-posta : ahmetdasdemir37@gmail.com

with those given in [5]. Further, in [7], Daşdemir also investigated the influence of arbitrarily inclined loading on the dependence between the dynamical behavior of a multi-layered system and the static initial stress force.

The second factor, i.e. geometry of problem, is another of the most decisive features that affect the dynamics of the deformable system. Here, a process in the construction of the body and the resultant body change the applied strategy for solving problems to be investigated. Therefore, there are many papers devoted to the solution to different problems today. For instance, in [8], Sergienko and Deineka solved an elasticity problem in a compound system with concentrated masses using the finite element method. In [9], Akbarov et al. investigated the axisymmetric vibration of an initially stressed bi-layered plate, under a harmonic point force, that rests on a rigid foundation. In [10], Zhuk and Guz analyzed the propagation of longitudinal and transverse plane waves in the pre-stressed layers of nanocomposites. In [11], Pandit et al. developed a new solution model for examining the buckling of the laminated slab with the transverse elastic core.

Based on current literature, it can be said that vibration by a time-harmonic force of an initially stressed slab resting on a rigid foundation made by compounding three materials side-by-side has not been studied so far. To fill this gap, a mathematical model for the mentioned problem is presented within the scope of a piecewise homogenous body model utilizing the framework of the TLTEWISB; moreover, this model is approximately solved using the finite element method (FEM). In particular, the effect of the initial stress on the frequency response of the slab is analyzed and discussed.

The paper is organized as follows. Section 2 introduces the general structures and features of our modal problem, while Section 3 describes the finite element method for forced vibration analysis of the composite slab with initial stress. Section 4 examines some concrete numerical examples. Section 5 summarizes some conclusions.

2. MODEL OF PROBLEM

Consider a pre-stressed tri-layered slab of thickness h and length $2a$ ($= r_1 + r_2 + r_3$), where r_1 , r_2 , and r_3 denote the length of layer in the left, middle and right side of the slab, respectively. The superscripts (1), (2), and (3) represent quantities corresponding to the left, middle, and right layers, respectively, and the values for the initial state are represented by the additional superscript "0".

The materials to be considered for the layers are moderately rigid, linear elastic, homogeneous, and isotropic. For an elastic medium, the stress-strain-displacement relationships are

$$\sigma_{ij}^{(m)} = \lambda^{(m)} \varepsilon_{ii}^{(m)} \delta_{ij} + 2\mu^{(m)} \varepsilon_{ij}^{(m)} \quad (1.a)$$

and

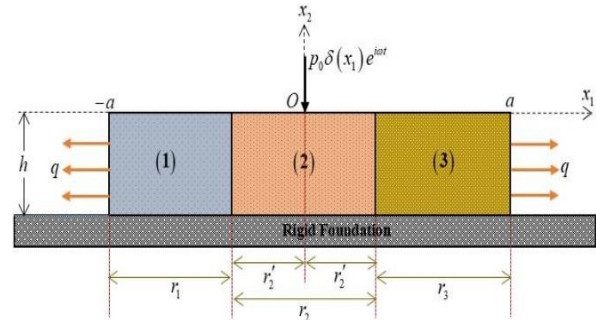


Figure 1. Scheme of the problem

$$\varepsilon_{ij}^{(m)} = (u_{i,j}^{(m)} + u_{j,i}^{(m)}) / 2, \quad (1.b)$$

where $m = 1, 2, 3$ and $i, j = 1, 2$. Moreover, $\sigma_{ij}^{(m)}$ are the stress components, $\varepsilon_{ij}^{(m)}$ are the strain components, and $u_i^{(m)}$ are the mechanical displacements of the slab. Here, $\lambda^{(m)}$ and $\mu^{(m)}$ are the Lamé constants, and δ_{ij} is the Kronecker delta. Further, the subscripts after commas represent the related coordinate differentiation. Note that in this equation and further in the document, repeated subscripts are summed over all possible values unless otherwise stated.

As Fig. 1 is shown, the compounded slab rests on a rigid foundation and has a lineal time-harmonic charge acting on the midpoint on the free surface of the middle layer. Note that this point is chosen as the origin of the coordinate system. It is assumed that there is the case of complete contact at the interfaces between the elastic layers. The positions of the points in the slab are identified by the Lagrangian coordinates denoted by x_i' , which in the unperturbed state overlap with Cartesian coordinates denoted by x_i . The body is infinitely long in the Ox_3 direction. Since the lineal force extends to infinity in this direction, however, the plane deformation state arises in the Ox_1x_2 plane, and therefore, all the numerical investigations are conducted in this plane. According to Fig. 1, the considered body occupies the domain of $D = D_1 \cup D_2 \cup D_3$, where

$$D_1 = \{(x_1, x_2) : -a \leq x_1 \leq -r_2', -h \leq x_2 \leq 0\}, \quad (2.a)$$

$$D_2 = \{(x_1, x_2) : -r_2' \leq x_1 \leq r_2', -h \leq x_2 \leq 0\}, \quad (2.b)$$

and

$$D_3 = \{(x_1, x_2) : r_2' \leq x_1 \leq a, -h \leq x_2 \leq 0\}, \quad (2.c)$$

respectively. Here, the prime indicates half of the corresponding length.

The process of creating the slab is as follows. First, the layers selected for creating the slab are compounded, and then the resultant system is exposed to homogeneously distributed normal forces (either tension or compression) before interacting with the rigid foundation. Note that the mentioned force is exactly static and applied to the

system according to the fundamental principle of TLTEWISB. Therefore, a uniaxial homogeneous initial stress state arises in the slab, which is determined as

$$\sigma_{11}^{(\ell),0} = q, \text{ and } \sigma_{ij}^{(\ell),0} = 0 \text{ for all } ij \neq 11, \quad (3)$$

where q is a certain constant and $l = 1, 3$.

Now, the equations of motion and the corresponding boundary-contact conditions related to the problem under consideration are modelled. According to the TLTEWISB, the general forms of the partial differential equations of motion can be expressed as follows [1-3]:

$$\sigma_{ij,j}^{(m)} + qu_{i,11}^{(m)} = \rho^{(m)} \ddot{u}_i^{(m)}, \quad (4)$$

where $\rho^{(m)}$ is the natural density of the corresponding layer. The dots over the quantities denote differentiation with respect to time.

Now the boundary-contact conditions for the considered problem are presented. Given above, they are as follows:

$$\sigma_{21}^{(m)} \Big|_{x_2=0} = 0, \quad \sigma_{22}^{(m)} \Big|_{x_2=0} = -p_0 \delta(x_1) e^{i\omega t}, \quad (5)$$

$$\sigma_{i2}^{(1)} \Big|_{x_1=-r_2'} = \sigma_{i2}^{(2)} \Big|_{x_1=-r_2'}, \quad \sigma_{i2}^{(2)} \Big|_{x_1=r_2'} = \sigma_{i2}^{(3)} \Big|_{x_1=r_2'}, \quad (6)$$

$$u_i^{(1)} \Big|_{x_1=-r_2'} = u_i^{(2)} \Big|_{x_1=-r_2'}, \quad u_i^{(2)} \Big|_{x_1=r_2'} = u_i^{(3)} \Big|_{x_1=r_2'}, \quad (7)$$

$$\left(qu_{j,1}^{(\ell)} + \sigma_{j1}^{(\ell)} \right) \Big|_{x_1=\pm a} = 0, \text{ and } u_j^{(m)} \Big|_{x_2=-h} = 0, \quad (8)$$

where $\delta(\cdot)$ is the Dirac's delta function.

The presentation of the problem is thereby exhausted.

3. SOLUTION TECHNIQUE

As the problem under consideration is quite complex, it cannot be solved analytically. Consequently, an approximate solution can be given by employing the FEM. To do this, certain preparations are needed to facilitate the solution process. First, introduce the dimensionless coordinate system

$$\hat{x}_1 = \frac{x_1}{h} \text{ and } \hat{x}_2 = \frac{x_2}{h}. \quad (9)$$

Since the force is a time-harmonic, with frequency ω , denoted by $p_0 \delta(x_1) e^{i\omega t}$, all the corresponding dependent variables can be represented as

$$\{ \sigma_{ij}, \varepsilon_{ij}, u_i \} (x_1, x_2, t) = \{ \bar{\sigma}_{ij}, \bar{\varepsilon}_{ij}, \bar{u}_i \} (x_1, x_2) e^{i\omega t}, \quad (10)$$

where the superimposed line over a quantity denotes its amplitude.

Substituting the expression in (10) into the foregoing equation and boundary terms after the transformation in (9), the equivalent equations and boundary-contact conditions are obtained for the amplitudes of the sought values by replacing the terms $\partial^2 u_i^{(m)} / \partial t^2$ and $p_0 \delta(x_1) e^{i\omega t}$ with $-\omega^2 u_j^{(m)}$ and $p_0 \delta(x_1)$, respectively. As a result, our original problem over the domain D takes shape the more simple form over the new domain

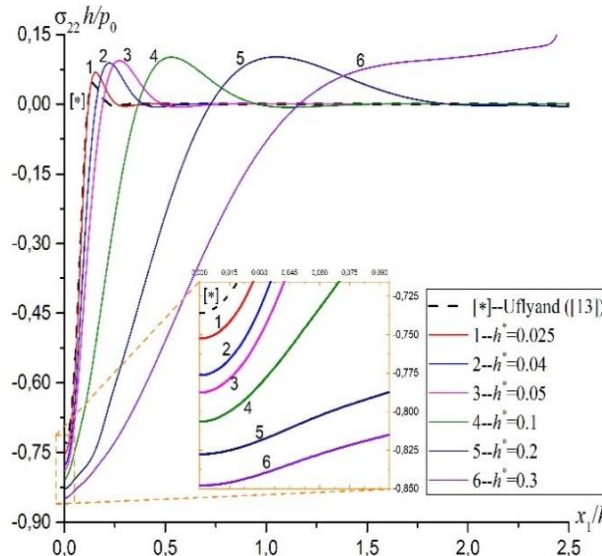


Figure 2. Convergence analysis for our algorithm

\bar{D} of unit thickness regardless of the time parameter t . Thereafter, the superimposed dashes and hats are neglected until specified otherwise.

To construct the FEM model of the last problem, the functional

$$J(\mathbf{u}^{(m)}) = \frac{1}{2} \int_D \left[T_{ij}^{(m)} u_{j,i}^{(m)} + (\Omega^{(m)})^2 (u_i^{(m)})^2 \right] dD + \int_{-a/h}^{a/h} \frac{p_0 \delta(x_1)}{\mu^{(m)}} u_2^{(2)} \Big|_{x_2=0} dx_1 \quad (11)$$

is proposed. Eq. (11) introduces the following notations:

$$T_{ij}^{(m)} = \frac{1}{\mu^{(m)}} \sigma_{ij}^{(m)} + \eta^{(m)} u_{j,n}^{(m)} = \frac{w_{ijkn}^{(m)}}{\mu^{(m)}} u_{n,k}^{(m)}, \quad (12)$$

$$\Omega^{(m)} = \omega h \sqrt{\rho^{(m)} / \mu^{(m)}}, \text{ and } \eta^{(m)} = q / \mu^{(m)}. \quad (13)$$

Here, $\Omega^{(m)}$ is the dimensionless frequency and $\eta^{(m)}$ is the initial stress parameter. From the mechanical relations in Eq. (1), the explicit forms of $w_{ijkn}^{(m)}$ in (12) are

$$\begin{aligned} w_{1111}^{(m)} &= \lambda^{(m)} + 2\mu^{(m)} + q, \quad w_{1122}^{(m)} = \lambda^{(m)}, \\ w_{1212}^{(m)} &= \mu^{(m)}, \quad w_{2121}^{(m)} = \mu^{(m)}, \\ w_{1221}^{(m)} &= \mu^{(m)} + q, \quad w_{2112}^{(m)} = \mu^{(m)}, \\ w_{2211}^{(m)} &= \lambda^{(m)}, \quad w_{2222}^{(m)} = \lambda^{(m)} + 2\mu^{(m)}. \end{aligned} \quad (14)$$

It should be noted that all the components, which cannot be visible in (14), are equal to zero. It is seen from Eq. (14) that the symmetry condition

$$w_{ijkn}^{(m)} = w_{nkji}^{(m)} \quad (15)$$

is satisfied.

The validity of the functional shown in Eq. (11) must be proven. Using the Gauss's theorem with the symmetry condition in (15) yields

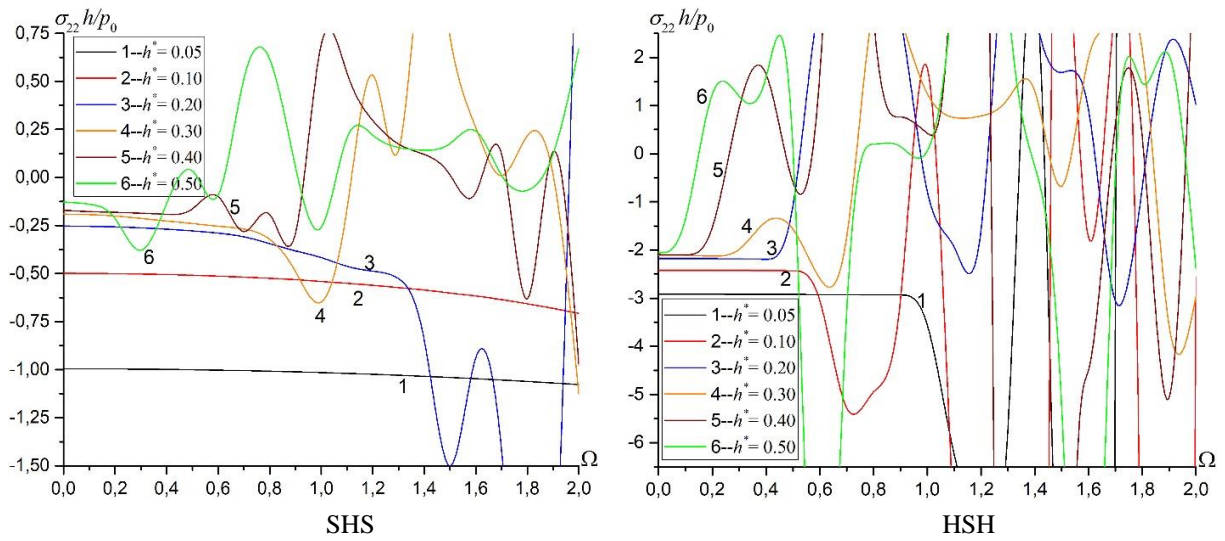


Figure 3. Dependence between $\sigma_{22}h / p_0$ and Ω for various values of h^*

$$\begin{aligned}
 \delta J(\mathbf{u}^{(m)}) &= \delta \left(\frac{1}{2} \int_D \left[\frac{w_{ijkn}}{\mu} u_{n,k} u_{j,i} + \Omega^2 (u_i)^2 \right] dD \right. \\
 &\quad \left. + \int_{-a/h}^{a/h} \frac{p_o \delta(hx_1)}{\mu} u_2 \right|_{x_2=0} dx_1 \Big) \\
 &= \frac{1}{2} \int_D \left[\frac{w_{ijnk} + w_{knji}}{\mu} u_{n,k} \delta u_{j,i} + 2\Omega^2 u_j \delta u_j \right] dD \\
 &\quad \left. + \int_{-a/h}^{a/h} \frac{p_o \delta(hx_1)}{\mu} u_2 \right|_{x_2=0} dx_1 \Big) \\
 &= \frac{1}{\mu} \int_D \left[w_{ijnk} u_{n,k} \delta u_{j,i} + \rho \omega^2 h^2 u_j \delta u_j \right] dD \\
 &\quad \left. + \int_{-a/h}^{a/h} \frac{p_o \delta(hx_1)}{\mu} u_2 \right|_{x_2=0} dx_1 \Big) \\
 &= -\frac{1}{\mu^{(m)}} \int_D \left[(w_{ijnk} u_{n,k})_{,i} - \rho \omega^2 h^2 u_j \right] \delta u_j dD \\
 &\quad \left. + \frac{1}{\mu} \int_S w_{ijnk} u_{n,k} \delta u_j n_i dS + \int_{-a/h}^{a/h} \frac{p_o \delta(hx_1)}{\mu} u_2 \right|_{x_2=0} dx_1 \Big)
 \end{aligned}$$

Here, S indicates the boundary of the slab and n_i are components of the unit normal vector on the boundary S . Note that the superscript “(m)” is omitted since the above equation contains large quantities. Finally, evaluating the equation “ $\delta J(\cdot) = 0$ ”, Eqs. in (4)-(8) are obtained, proving the validity of the functional in (11).

Now, the FEM model for the considered problem is constructed using the virtual work principle and the Ritz method [12]. To do this, the domain D is split into a finite number of smaller piecewise consisting of nine-node smooth rectangular elements. A sufficient number of finite elements is required to satisfy the boundary-contact terms with high precision and to ensure very well

approximation of the numerical results. Let the displacement components for the finite element be

$$u_1^{(k)} = \sum_{i=1}^M c_i^{(k)} N_i(r, s) \text{ and } u_2^{(k)} = \sum_{i=1}^M d_i^{(k)} N_i(r, s), \quad (16)$$

where M is the number of the nodes in the k th element, the coefficients $c_i^{(k)}$ and $d_i^{(k)}$ are unknowns that need to be determined, r and s are local space components over a finite element, and $N_i(r, s)$ are the interpolation polynomials for the k th element. In this study, the interpolation functions are selected such as $N_i(r, s) \in L^2$, where L^2 is a set of Lebesgue integrable functions.

Substituting Eqs. (16) into Eq. (11) and applying the usual solution method to the resultant equation leads to a matrix system as

$$(\mathbf{K} - \omega^2 \mathbf{M}) \mathbf{U} = \mathbf{R}, \quad (17)$$

where \mathbf{K} is the structure matrix, \mathbf{M} is the mass matrix, \mathbf{U} is the vector of unknowns, and \mathbf{R} is the load vector. To diminish the volume of the current paper the explicit entries of matrices and vectors in (17) are not given here. But, one can obtain their explicit forms from Eqs. (11)-(15) using this procedure. The displacements at the nodes can now be obtained by solving the matrix equation (17). As a result, these can easily be transformed into the corresponding stress values via the stress-strain matrix relationship.

This exhausts the presentation of the FEM model for the problem.

4. NUMERICAL FINDINGS AND DISCUSSIONS

This section presents some numerical results. First, some explanations to be needed are made. The number of the finite element was chosen such that 200 and 80 along the

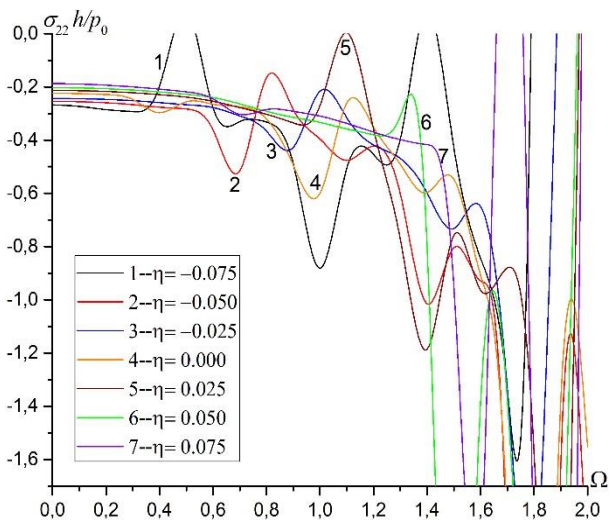


Figure 4. Dependence between $\sigma_{22}h / p_0$ and Ω for various values of h^*

Ox_1 , and Ox_3 axes, respectively. All the algorithms needed to obtain numerical solutions were done in Mathematica[®] software. Using these numerical results, the original figures are designed in OriginPro[®] program. Note that the global node numbers are aligned from the below to the above. This selection provides us certain advantages. Since the force applied to the body under consideration is perpendicular to its free surface, the graphs are symmetrical about the line x_1 / h . Even though it is possible to draw the graphs to be investigated in anywhere of the slab using our PC algorithm, throughout the paper, the numerical results will be given at the interface between the slab and the rigid foundation and in the parts of the diagrams where $x_1 / h \geq 0$.

Introduce the notations

$$h^* = h / 2a, \quad r_* = r_1 / r_2, \quad \text{and} \quad e_{mn} = E^{(m)} / E^{(n)}, \quad (18)$$

where r_* is the ratio of the layer length, h^* is the thickness ratio, $E^{(m)}$ is the Young's Modulus of the m th layer, and e_{mn} is the ratio of the layer's Young's Modulus. For simplicity, all the numerical investigations are given under $h^* = 0.2$, $r_1 = r_2 = r_3$, $\Omega^{(m)} = 0$, and $\eta^{(m)} = 0$ unless otherwise specified. Hereafter, all the superscripts of the parameters that have equal values will be neglected. To investigate the concrete examples, the following cases are investigated: (i) Al+St+Al, and (ii) St+Al+St, as investigated by Daşdemir and Eröz [7], where Al and St indicate abbreviations of Aluminium and Steel materials, respectively.

Before giving our numerical results, the accuracy and trustiness of the PC algorithm composed of the current problem must be proven. For validation purposes, consider the case with $e_{mn} = 1$, $\nu^{(1)} = \nu^{(2)} = \nu^{(3)} = 0.33$ in addition to the above assumptions, where $\nu^{(m)}$ is the

Poisson ratio for m th layer. Here, for $h^* \rightarrow 0$, the

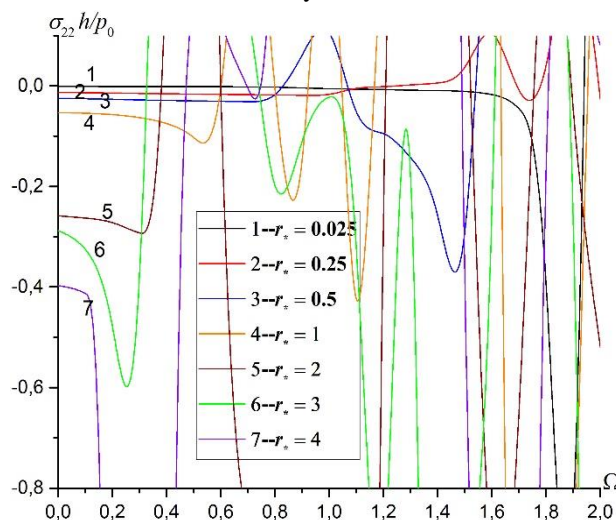


Figure 5. Dependence between $\sigma_{22}h / p_0$ and Ω for various values of r_*

geometry of the problem resembles the one investigated by Uflyand [13] for an infinitely long plate. Our numerical results, therefore, must approach those of [13]; and the graphs in Fig. 2 show that this is the case. Thus, the validity and reliability of the algorithms were demonstrated. Note that the starred graph denotes the one presented in [13].

The main aim of the paper is to obtain the numerical results illustrating the effects of the corresponding problem parameters on the frequency response of the slab. For this purpose, all subsequent numerical investigations will be conducted at the point (0,- 1) for both Case 1 and Case 2; this will not impair the generality of the results.

In Fig. 3, variations of the normal stress $\sigma_{22}h / p_0$ versus dimensionless frequency Ω for both Case 1 (Fig. 3a) and Case 2 (Fig. 3b) for various values of the thickness ratio h^* is displayed. The dependence between $\sigma_{22}h / p_0$ and Ω is non-monotonous. The stress becomes damp as h^* increases. It is concluded from the graphs that there are some points the stress $\sigma_{22}h / p_0$ has maximal or minimal values. These are called resonance values of stress and indicated by Ω^* . The values of Ω^* can be detected from each graph. According to the distributions of graphs in Fig. 3, the values of Ω^* decrease as h^* increases. It is clear that the choice of the layers such that Soft+Hard+Soft (SHS) is more ideal than that of Hard+Soft+Hard (HSH); accordingly, only the case SHS will be considered after this. This means that the resonance values depend on the material selections of the layers as well as the thickness ratio. In addition, an increase in the values of h^* leads to a decrease in the number of extreme of $\sigma_{22}h / p_0$.

Now, the effect of the initial stress parameter η at the layers is focused on the frequency response of the system,

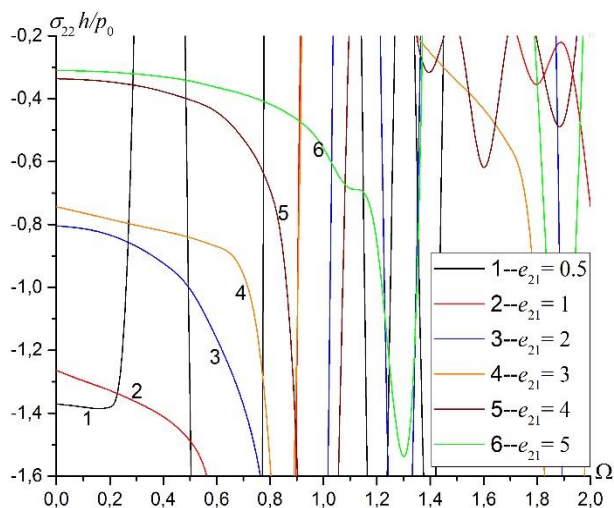


Figure 6. Dependence between $\sigma_{22}h/p_0$ and Ω for various values of the ratio e_{21}

considering the graphs in Fig. 4. According to the numerical results, it is concluded that while the initial tension causes to increase the absolute values of $\sigma_{22}h/p_0$, the initial compression has an opposite effect. At the same time, an increase in the value of the initial stress parameter η leads to obtain a more stable system, giving rise to increasing the values of Ω^* . Further, it is clear that the slab has local parametric resonances, denoted by Ω^{**} , for certain values of the initial stress parameter η , e.g. for $\eta=0$, $\Omega^{**} \approx 0.35$. The distributions of the graphs in Fig. 4 prove that the number of the extreme values of $\sigma_{22}h/p_0$ decreases as the values of η increases. The conclusion is that the effect of the parameter η on the values of Ω^* is notable not only quantitatively, but also qualitatively. The parameter η has a great influence on the resonance mode of $\sigma_{22}h/p_0$. In the manufacture of the material, not only the selection of materials for the layers but also the design of layers is an important issue.

Fig. 5 provides us the facility to investigate the effect of the ratio of the layer length on the frequency response of the slab. The absolute values of $\sigma_{22}h/p_0$ decrease gradually with the ratio r_* . An increase in the value of the layer length ratio r_* causes to decrease the resonance values of the slab; namely, when the length of the soft layer is relatively smaller than that of the hard part, the stability of the system under consideration increases. As a result, it can be said from the numerical results in Figs. 4 and 5 that the values of Ω^* are considerably affected by not only the initial stress parameter η but also the layer length ratio r_* . Note that the number of the maxima and minima values of $\sigma_{22}h/p_0$ decrease accordingly with the ratio r_* .

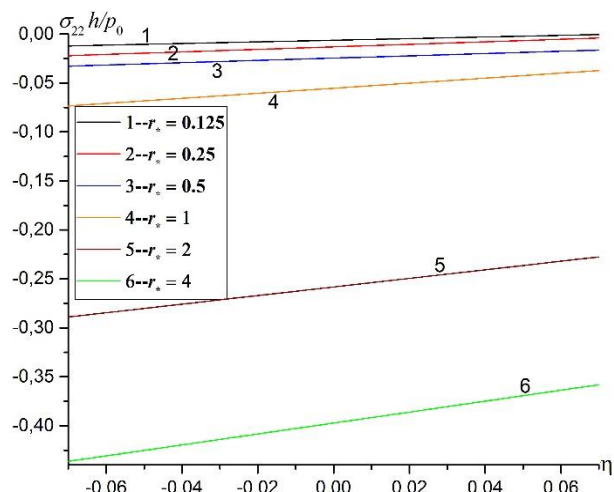


Figure 7. Dependence between $\sigma_{22}h/p_0$ and η for various values of the ratio r_*

Now, consider the case where $\nu^{(1)} = \nu^{(2)} = \nu^{(3)} = 0.33$. In this situation, Fig. 6 allows us to observe the influence of the ratio of Young's modulus e_{21} on the relationships between $\sigma_{22}h/p_0$ and Ω . It is evident from the graphs that an increase in the value of the ratio e_{21} prevents the resonance mode of the slab. This means that the stability of the system under consideration increases with the ratio e_{21} . Further, the number of extreme values of the normal stress $\sigma_{22}h/p_0$ versus Ω decreases as the ratio e_{21} increases. By the way, the results obtained from the figure agree well with the well-known mechanical findings, again proving the validity and the trustworthiness of the PC algorithm.

The foregoing numerical results were discussed without reference to the initial stress state in the slab up to now, namely $\eta^{(m)} = 0$. But, one of the principal goals of the paper is to investigate the influence of the mentioned state on the dynamic behavior of the slab. For this purpose, Fig. 7 shows the variations of the stress $\sigma_{22}h/p_0$ with respect to η for certain values of the ratio r_* . According to the graphs, the values of $\sigma_{22}h/p_0$ changes linearly with η . While an increase in the value of the initial compression parameter η causes to increase the value of $\sigma_{22}h/p_0$, the increasing value of the initial tension parameter η leads contrarily to decrease the stress $\sigma_{22}h/p_0$. The ratio r_* has a significant role in the influence of the initial stress parameter η on the dynamic behavior of the slab. Indeed, the decreasing value of the ratio r_* causes to damp the influence of η on the values of $\sigma_{22}h/p_0$.

5. CONCLUSIONS

In this paper, the forced vibration induced by a time-harmonic external force of a pre-stressed slab with three

compressible layers, which rest on a rigid foundation, has been investigated. This has been made based on the fundamental principles of the TLTEWISB in the case where there exists a complete contact interaction between the layers. The mathematical problem is created under consideration and numerically solved using the FEM. Numerical results have demonstrated the influence of the design of the body on the frequency response of the normal stress, acting on the interface planes between the slab and rigid foundation. Numerical investigations have shown the following:

- an increase in the values of the initial stress parameter η causes the resonance mode of the normal stress $\sigma_{22}h / p_0$ to vanish;
- the choice of the materials for the layers has a great influence on the frequency response of $\sigma_{22}h / p_0$;
- the values of Ω^* decrease as the values of the ratio r_* increase;
- the numbers of the local maxima and minima of the stress $\sigma_{22}h / p_0$ versus the dimensionless frequency Ω decrease with increasing the ratio r_* ;
- and the influence of η on the stress distributions in the slab damps as the values of the ratio r_* decreases.

ACKNOWLEDGEMENTS

The author would like to acknowledge the financial grant given by the Research Fund of Kastamonu University for this research through the project KÜBAP-01/2016-04.

DECLARATION OF ETHICAL STANDARDS

The author(s) of this article declare that the materials and methods used in this study do not require ethical committee permission and/or legal-special permission.

NOMENCLATURE

- a : length of the slab
- Al : Aluminum
- $c_i^{(k)}, d_i^{(k)}$: nodal unknowns
- D : the domain of the slab
- D_1, D_2, D_3 : domains of the layers
- e_{mn} : the ratio of Young's modulus of m th and n th layer material
- $E^{(m)}$: Young's modulus of m th layer
- FEM : finite element method
- h : the thickness of the slab
- h^* : thickness ratio
- $J(\mathbf{u}^{(m)})$: the total potential energy functional

- \mathbf{K} : structure matrix
- L_2^1 : the set of Lebesgue integrable functions
- $\square^{(m)}$: m th layer in slab
- M : the number of the nodes over a finite element
- \mathbf{M} : mass matrix
- n_i : components of the unit normal vector
- $N_{ij}(r, s, t)$: the shape functions
- O : origin of the coordinate system
- p_0 : value of dynamic force
- $q_{ij}^{(m)}$: value of initial stress of m th layer
- r_* : the ratio of the layer length
- r_1, r_2, r_3 : the lengths of layer
- r, s : local normalized coordinate components
- R : work of the external force
- \mathbf{R} : load vector
- S : boundary of slab
- St : Steel
- TLTEWISB : three-dimensional linearized theory of elastic waves in initially stressed bodies
- $u_i^{(m)}$: components of the displacement vector
- \mathbf{U} : nodal displacement vector
- x_i : Cartesian coordinate components
- x_i' : Lagrange coordinate components
- \hat{x}_i : Normalized coordinate components
- δ : variation parameter
- δ_{ij} : Kronecker delta
- $\delta(\cdot)$: Dirac's delta function
- $\varepsilon_{ij}^{(m)}$: strain tensor of m th layer
- $\eta^{(m)}$: initial stress parameter of the m th layer
- $\lambda^{(m)}, \mu^{(m)}$: Lamé constants
- $\nu^{(m)}$: Poisson ratio of m th layer
- $\rho^{(m)}$: the mass density of m th layer
- $\sigma_{ij}^{(m)}$: components of the stress tensor
- $\sigma_{ij}^{(m),0}$: initial stress acting in the layers
- ω : frequency of the external force
- $\Omega^{(m)}$: dimensionless frequency
- Ω^* : resonance value
- Ω^{**} : local parametric resonance value

REFERENCES

[1] Guz A.N., "Fundamentals of the Three-dimensional Theory of Stability of Deformable Bodies", (trans. from

- Russian by M. Kashtalian), Springer-Verlag, New York, (1999).
- [2] Akbarov S.D., “*Stability Loss and Buckling Delamination: Three-Dimensional Linearized Approach for Elastic and Viscoelastic Composites*”, Springer-Verlag, New York, (2013).
- [3] Akbarov S.D., “*Dynamics of Pre-Strained Bi-Material Elastic Systems: Linearized Three-Dimensional Approach*”, Springer-Verlag, New York, (2015).
- [4] Wen-tao H., Tang-dai X., Wei-yun C., “Influence of lateral initial pressure on axisymmetric wave propagation in hollow cylinder based on first power hypo-elastic model”, *Journal of Central South University*, 21(2): 753-760, (2014).
- [5] Daşdemir A., Eröz M., “Mathematical modeling of dynamical stress field problem for a pre-stressed bi-layered plate-strip”, *Bulletin of the Malaysian Mathematical Sciences Society*, 38(2): 733-760, (2015).
- [6] Daşdemir A., “Dynamic response of a pre-stressed bi-layered plate-strip subjected to an arbitrary inclined time-harmonic force”, *Creative Mathematics and Informatics*, 26(3): 255-262, (2017).
- [7] Daşdemir A., “Effect of initial stress on the dynamic response of a multi-layered plate-strip subjected to an arbitrary inclined time-harmonic force”, *International Journal of Applied Mechanics and Engineering*, 22(3): 521-537, (2017).
- [8] Sergienko I.V., Deineka V.S., “Numerical solution of the dynamic problem of elasticity for bodies with concentrated masses”, *International Applied Mechanics*, 40(12): 1360-1370, (2004).
- [9] Akbarov S.D., Zamanov A.D., Suleimanov T.R., “Forced vibration of a prestretched two-layer slab on a rigid foundation”, *Mechanics of Composite Materials*, 41(3): 229-240, (2005).
- [10] Zhuk Y.A., Guz I.A., “Features of propagation of plane waves along to the layers of an initially stressed nanocomposite material”, *International Applied Mechanics*, 43(4): 3-26, (2007).
- [11] Pandit M.K., Singh B.N., Sheikh A.H., “Buckling of laminated sandwich plates with soft core based on an improved higher order zigzag theory”, *Thin-Walled Structures*, 46(11): 1183-1191, (2008).
- [12] Zienkiewicz O.C., Taylor R.L., “*The Finite Element Method, Basic Formulation and Linear Problems*”, McGraw-Hill, London, (1989).
- [13] Uflyand Ya.S., “*Integral Transformations in the Theory of Elasticity*”, Nauka, Moscow-Leningrad, (1963).